

Electronic Supplementary Information

Experimental section

Materials: Cobalt nitrate hexahydrate ($\text{Co}(\text{NO}_3)_2 \cdot 6\text{H}_2\text{O}$), nickel nitrate hexahydrate ($\text{Ni}(\text{NO}_3)_2 \cdot 6\text{H}_2\text{O}$), Iron(III) nitrate nonahydrate ($\text{Fe}(\text{NO}_3)_3 \cdot 9\text{H}_2\text{O}$), and nitric acid (HNO_3) were obtained from Chengdu Kelong Chemical Reagent Factory. Ruthenium oxide (RuO_2), ammonium fluoride (NH_4F), urea, ethanol ($\text{C}_2\text{H}_5\text{OH}$), sodium chloride (NaCl), sodium carbonate (Na_2CO_3), and KOH were purchased from Aladdin Ltd. (Shanghai, China). Nafion (5 wt%) was purchased from Sigma-Aldrich Chemical Reagent Co., Ltd. Carbon cloth (CC) was provided by Hongshan District, Wuhan Instrument Surgical Instruments business. Natural seawater was collected from Weihai, Shandong, China, and most of the magnesium and calcium salts were removed by first adding 3.4 g Na_2CO_3 to 500 mL of natural seawater before use. All the reagents were used as received without further purification and the water used throughout all experiments was purified through a Millipore system (18.25 M Ω .cm).

Preparation of CoS_2/CC : A piece of CC with a size of $2 \times 2 \text{ cm}^2$ was cleaned in ethanol and HNO_3 for 15 min. After that, cleaned ultrasonically in deionized water for 15 min. $\text{Co}(\text{NO}_3)_2 \cdot 6\text{H}_2\text{O}$ (0.45 g), NH_4F (0.15 g), and urea (0.45 g) were dissolved in 30 mL water and stirred for 30 min, which was then transferred to a Teflon reactor with CC to be incubated at 120 °C for 6 h in a dry oven. After cooling down to room temperature, the $\text{Co}(\text{OH})\text{F}/\text{CC}$ was acquired. To obtain CoS_2/CC , the precursor $\text{Co}(\text{OH})\text{F}/\text{CC}$ and S powder (2 g) were placed at two separate positions in one porcelain boat with S powder at the upstream side of the furnace. Subsequently, the sample was heated at 400 °C for 2 h with a heating speed of 2 °C min^{-1} under Ar. The furnace was then allowed to cool to room temperature in Ar.

Preparation of $\text{CoS}_2@\text{NiFe-LDH}/\text{CC}$ and $\text{NiFe-LDH}/\text{CC}$: For the synthesis of $\text{CoS}_2@\text{NiFe-LDH}/\text{CC}$, Ag/AgCl (saturation KCl solution), CoS_2/CC , and Pt column were served as the reference electrode, working electrode, and counter electrode, respectively. Typically, 2.181 g of $\text{Ni}(\text{NO}_3)_2 \cdot 6\text{H}_2\text{O}$ and 2.085 g of $\text{Fe}(\text{NO}_3)_3 \cdot 9\text{H}_2\text{O}$ were dissolved in an electrolytic bath, the potential is -1 V vs. Ag/AgCl and the optimal

deposition time is 50 s. NiFe-LDH/CC was similarly prepared using CC as the working electrode. The loading masses of CoS₂@NiFe-LDH and NiFe-LDH are 3.50 and 2.81 mg/cm², respectively.

Preparation of RuO₂/CC: 5 mg RuO₂ (or 20% Pt/C) was added in a solution containing 30 μL of Nafion, 485 μL of ethanol, and 485 μL of deionized water with the aid of ultrasonication (30 min) to form a homogeneous ink (5 mg mL⁻¹). 350 μL of catalyst ink was dropped onto a piece of clean CC (1.0 × 0.5 cm²).

Characterizations: X-ray diffraction (XRD) patterns were collected by using a LabX XRD-6100 X-ray diffractometer with a Cu Kα radiation (40 kV, 30 mA) of wavelength 0.154 nm (SHIMADZU, Japan). X-ray photoelectron spectra (XPS) were obtained with an ESCALABMK II X-ray photoelectron spectrometer using a nonmonochromatized Al Kα X-ray source (1486.6 eV). Scanning electron microscopy (SEM) images were collected on a Helios G4 UC scanning electron microscope (Thermo Fisher Scientific). Transmission electron microscopy (TEM) images were obtained by using a HITACHI H-8100 electron microscopy (Hitachi, Tokyo, Japan) operated at 200 kV.

Electrochemical measurements: Electrochemical measurements were performed with a CHI 660E electrochemical analyzer in a standard three-electrode system, consisting of the CoS₂@NiFe-LDH/CC working electrode, carbon rod counter electrode, and Hg/HgO reference electrode. Electrochemical tests of OER activity were performed under alkaline conditions (1 M KOH, 1 M KOH + 0.5 M NaCl, and 1 M KOH + seawater). All measured potentials were calibrated to a reversible hydrogen electrode (RHE) using the following formula: $E(\text{RHE}) = E(\text{Hg/HgO}) + 0.059 \times \text{pH} + 0.098$. The LSV curves were obtained from 1.0 to 1.8 V vs. RHE. The electrochemical impedance spectroscopy (EIS) analysis was performed at the open circuit potential from 10000 to 0.01 Hz at an amplitude of 5 mV. The Faradaic efficiency (FE) of OER was determined using the drainage method in a two-compartment H-type cell, which was separated by a Nafion 117 membrane. Electrochemical active surface area (ECSA) was measured by Cyclic voltammetry (CV) with different scan rates of 20, 40, 60, 80, and 100 mV s⁻¹. The ECSA of the catalyst can be calculated by using the following equation:

$$\text{ECSA} = S_{\text{geometric area}} \times C_{\text{dl}}/C_{\text{S}}$$

Where C_{dl} is the experimentally obtained capacitance, C_{S} is the specific capacitance, and $S_{\text{geometric area}}$ is the geometric area of the electrode.

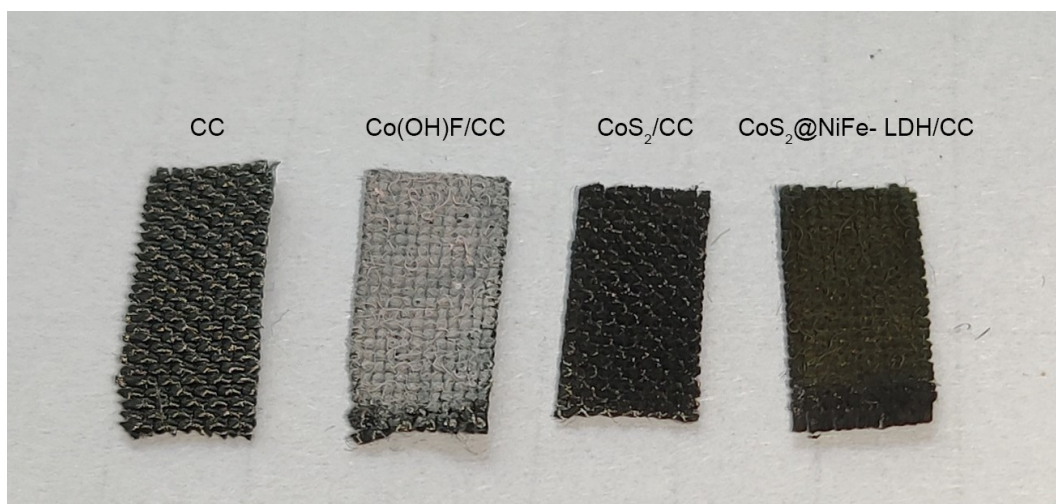


Fig. S1. Digital photograph of bare CC, Co(OH)F/CC, CoS₂/CC, and CoS₂@NiFe-LDH/CC.

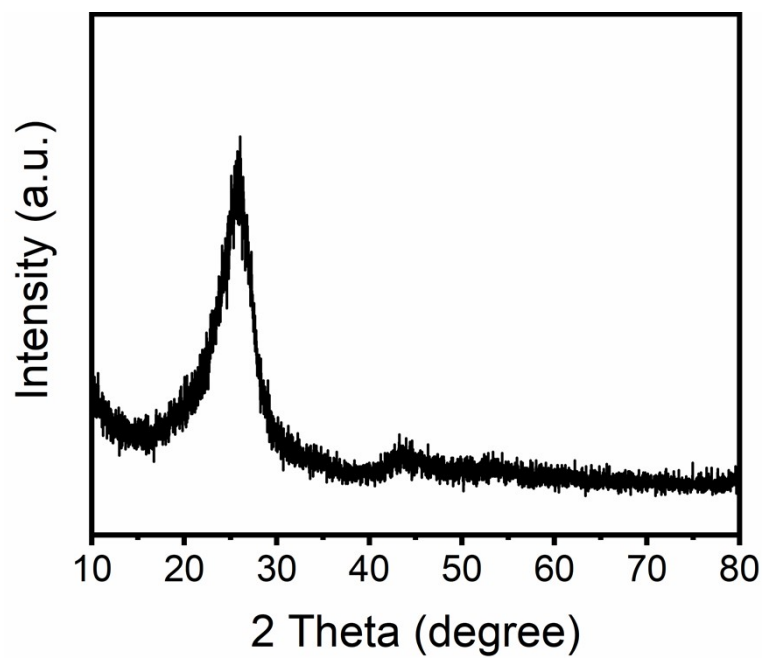


Fig. S2. XRD pattern of bare CC.

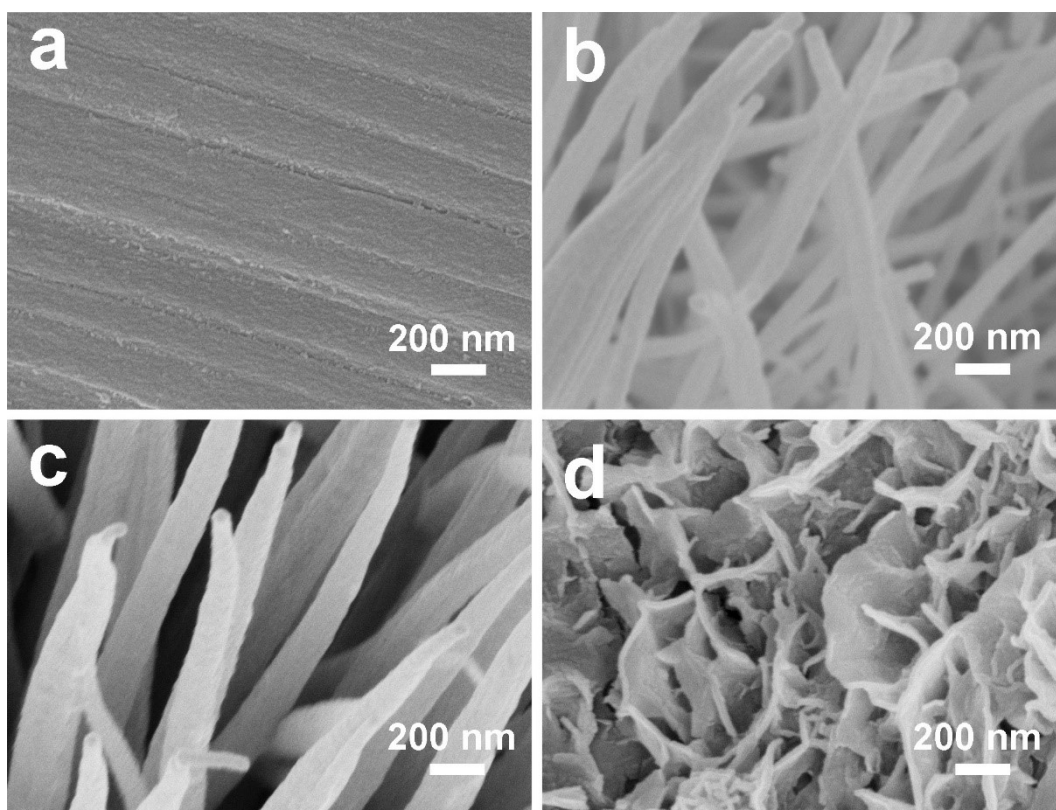


Fig. S3. SEM images of (a) bare CC, (b) Co(OH)F/CC, (c) CoS₂/CC, and (d) NiFe-LDH/CC.

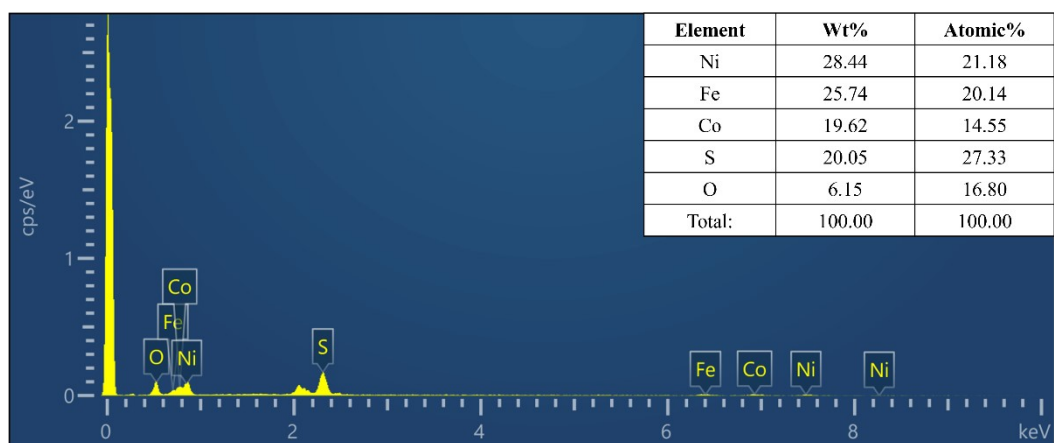


Fig. S4. EDX spectrum of CoS₂@NiFe-LDH/CC.

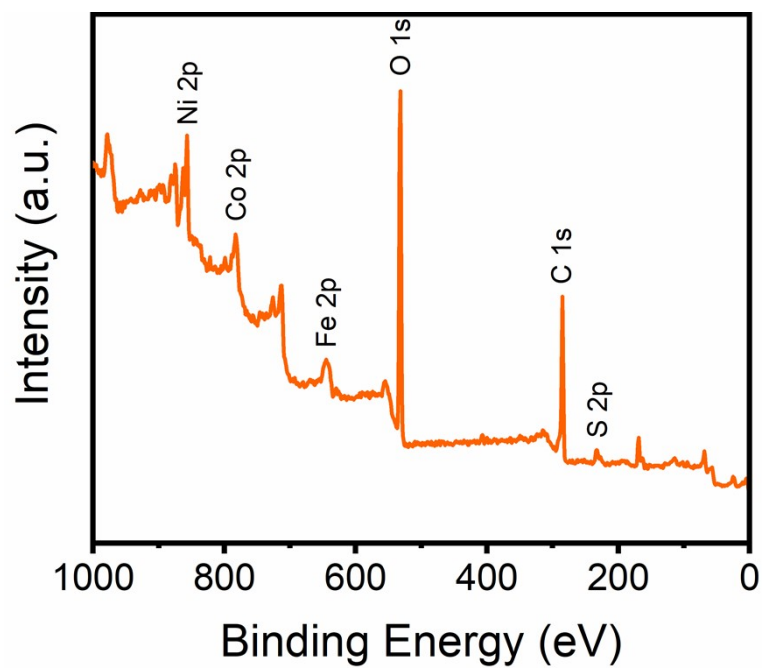


Fig. S5. XPS survey spectrum of $\text{CoS}_2@\text{NiFe-LDH/CC}$.

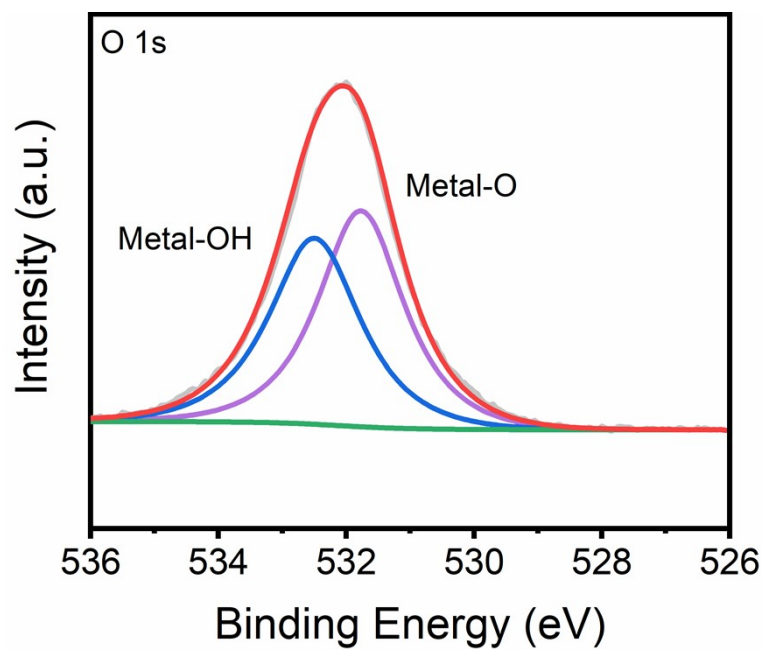


Fig. S6. High-resolution XPS spectrum of CoS₂@NiFe-LDH/CC in O 1s region.

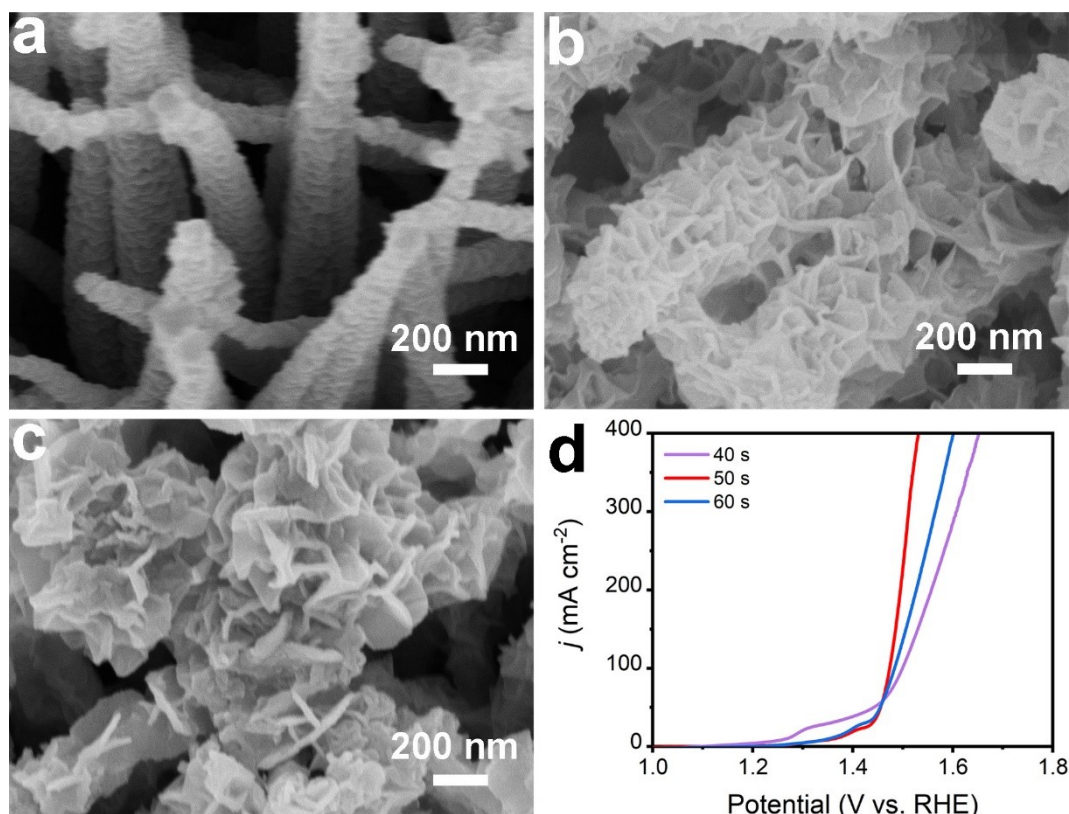


Fig. S7. SEM images for CoS₂@NiFe-LDH/CC at different deposition times of (a) 40 s, (b) 50 s, and (c) 60 s. (d) Corresponding LSV curves of CoS₂@NiFe-LDH/CC at different deposition times in 1 M KOH.

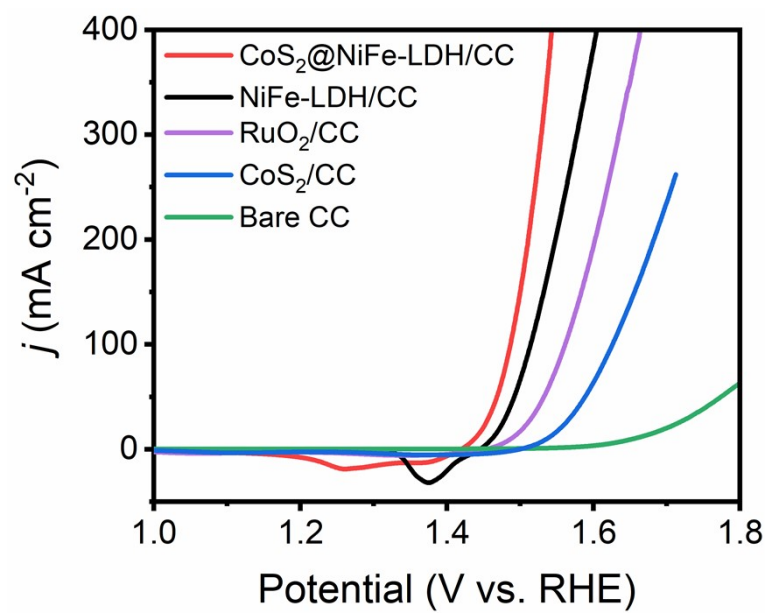


Fig. S8. LSV curves for $\text{CoS}_2@NiFe-LDH/CC$, $NiFe-LDH/CC$, CoS_2/CC , RuO_2/CC , and bare CC scanned from 1.8 V to 1.0 V in 1 M KOH.

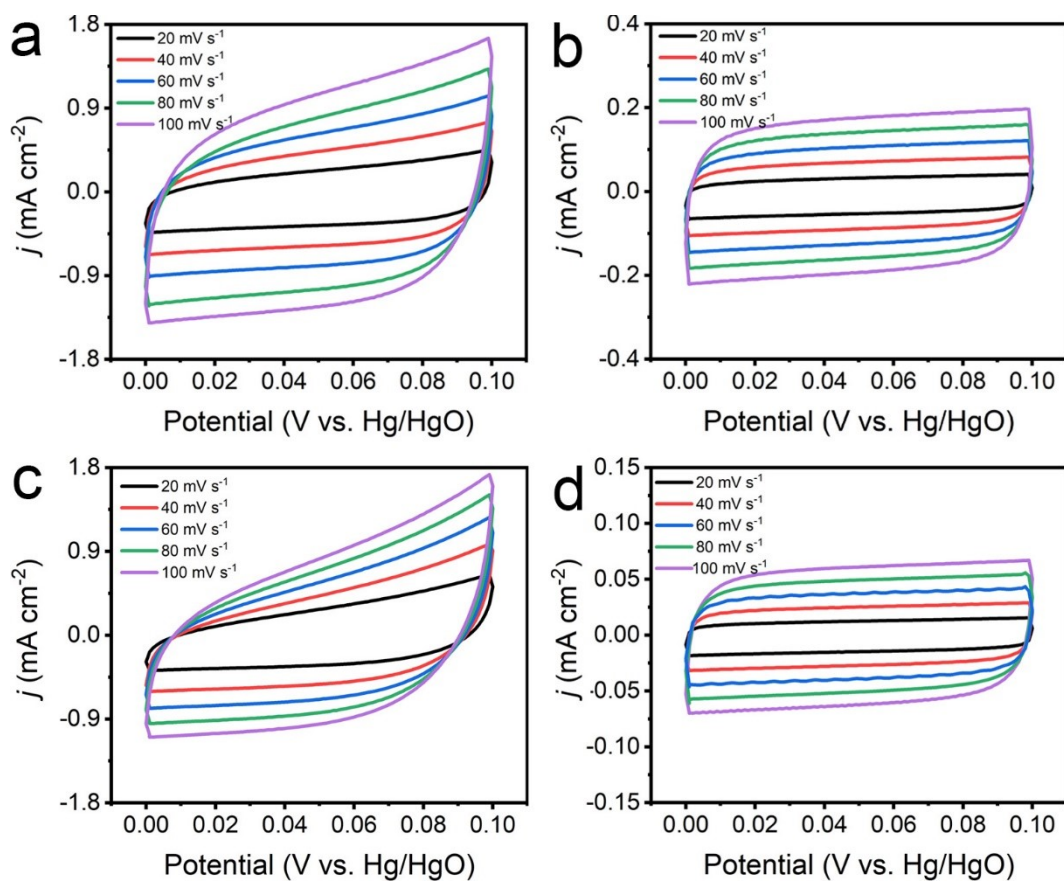


Fig. S9. Cyclic voltammety curves for (a) CoS₂@NiFe-LDH/CC, (b) NiFe-LDH/CC (c) CoS₂/CC, and (d) bare CC in the double layer region at different scan rates of 20, 40, 60, 80, and 100 mV s⁻¹ in 1 M KOH.

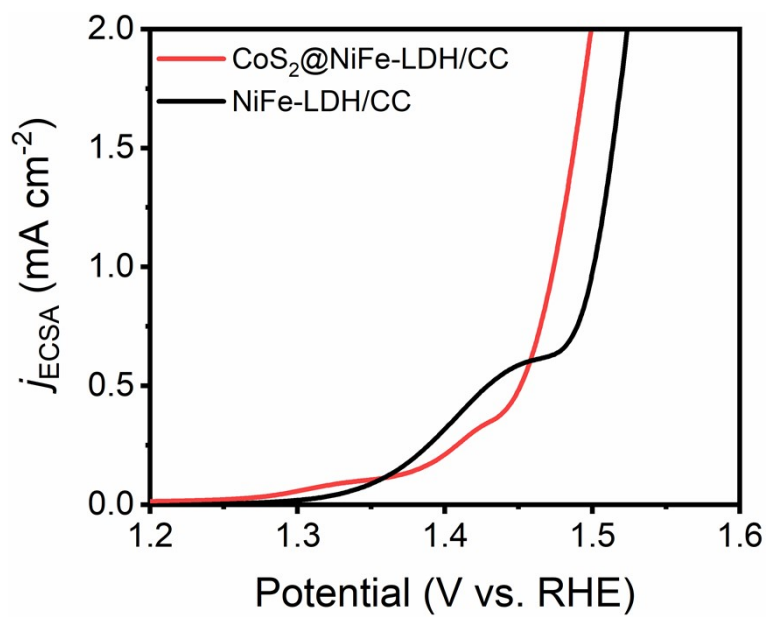


Fig. S10. ECSA-normalized LSV curves for CoS₂@NiFe-LDH/CC and NiFe-LDH/CC in 1 M KOH.

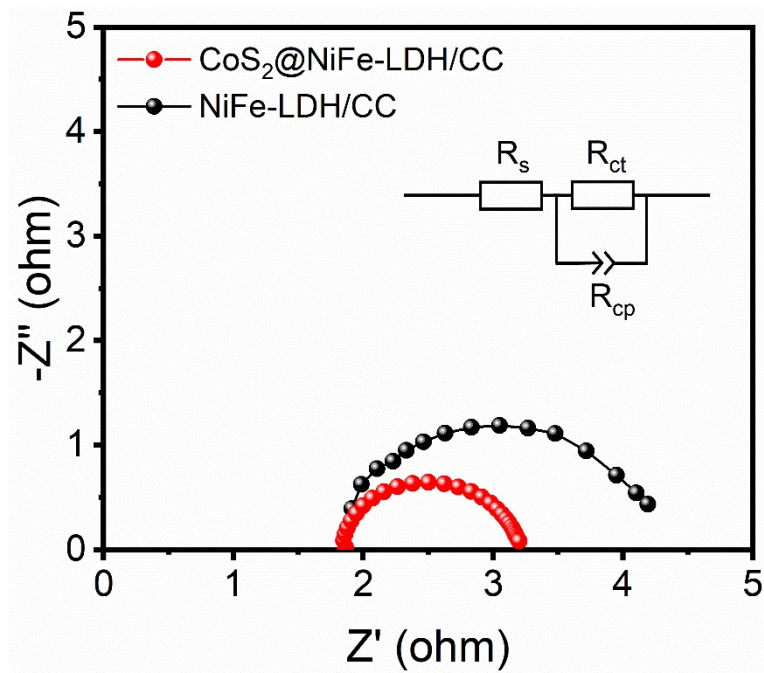


Fig. S11. Nyquist plots for $\text{CoS}_2@NiFe-LDH/CC$ and $NiFe-LDH/CC$.

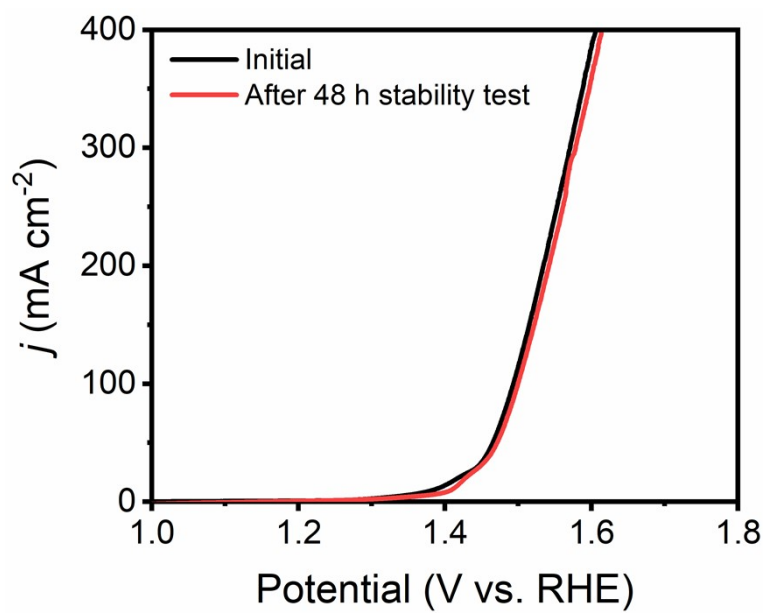


Fig. S12. LSV curves of CoS₂@NiFe-LDH/CC before and after 48 h stability test at the j of 100 mA cm⁻² in 1 M KOH + Seawater.

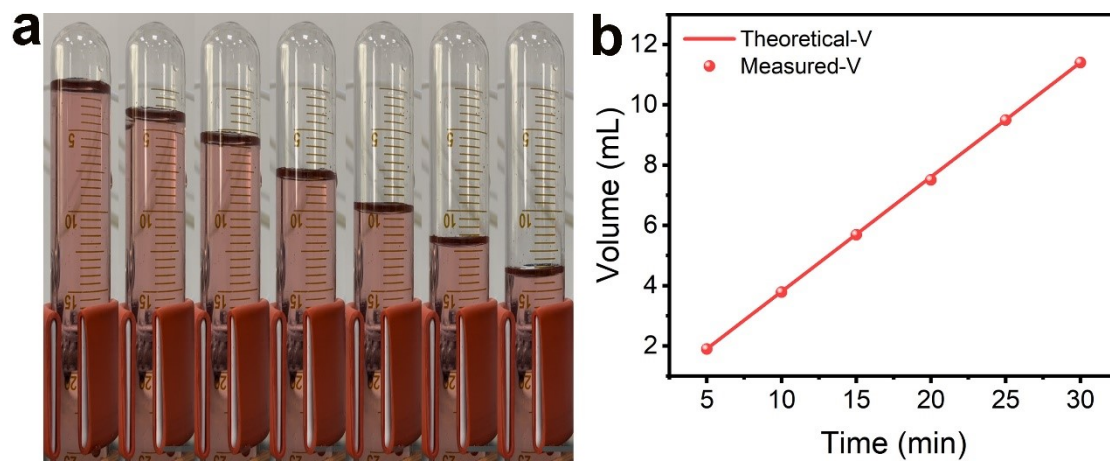


Fig. S13. (a) Digital photographs of the collected O_2 and (b) comparison between the amount of collected and theoretical O_2 for $CoS_2@NiFe-LDH/CC$ at a j of 100 mA cm^{-2} in 1 M KOH + Seawater.

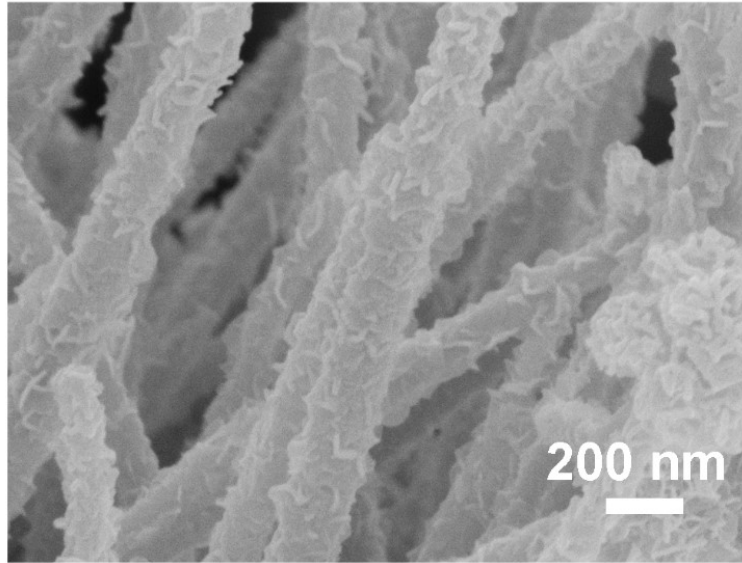


Fig. S14. SEM image of CoS₂@NiFe-LDH/CC after durability test in 1 M KOH + Seawater.

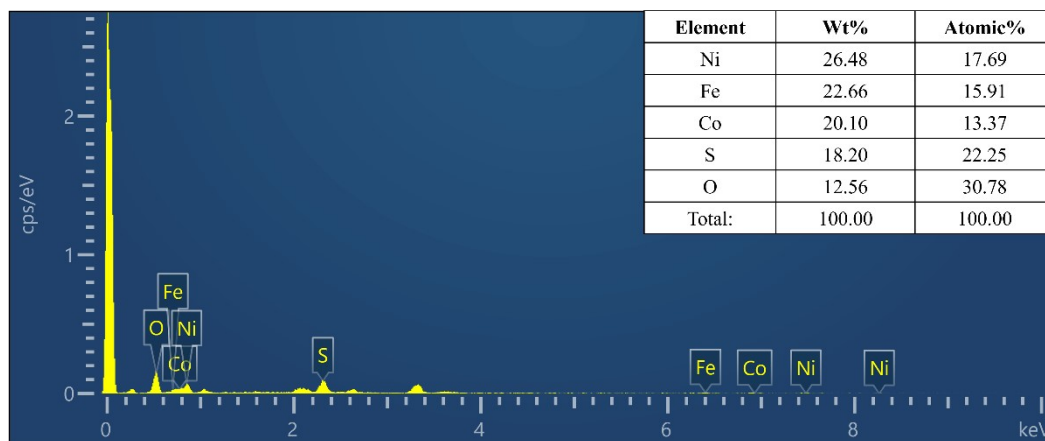


Fig. S15. EDX spectrum of $\text{CoS}_2@\text{NiFe-LDH/CC}$ after durability test in 1 M KOH + Seawater.

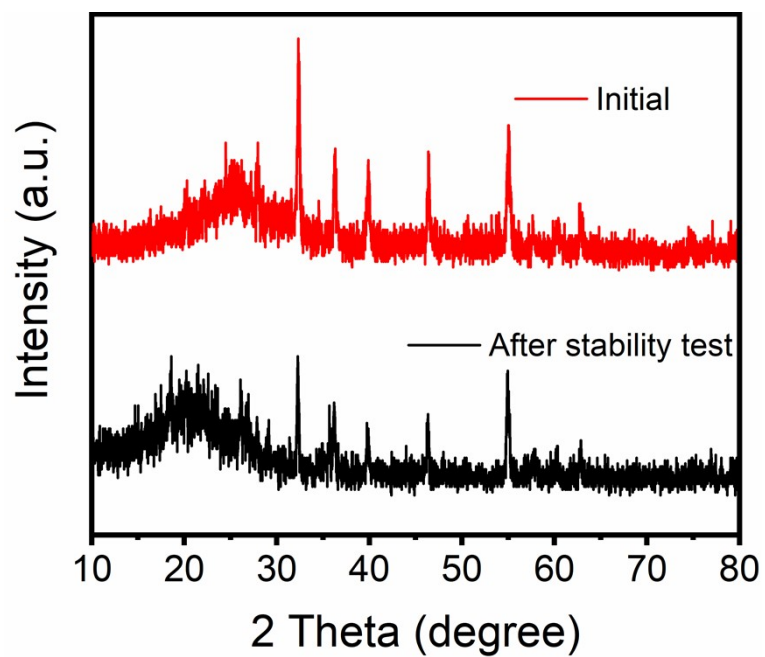


Fig. S16. XRD patterns of $\text{CoS}_2@\text{NiFe-LDH/CC}$ before and after OER stability test in 1 M KOH + Seawater.

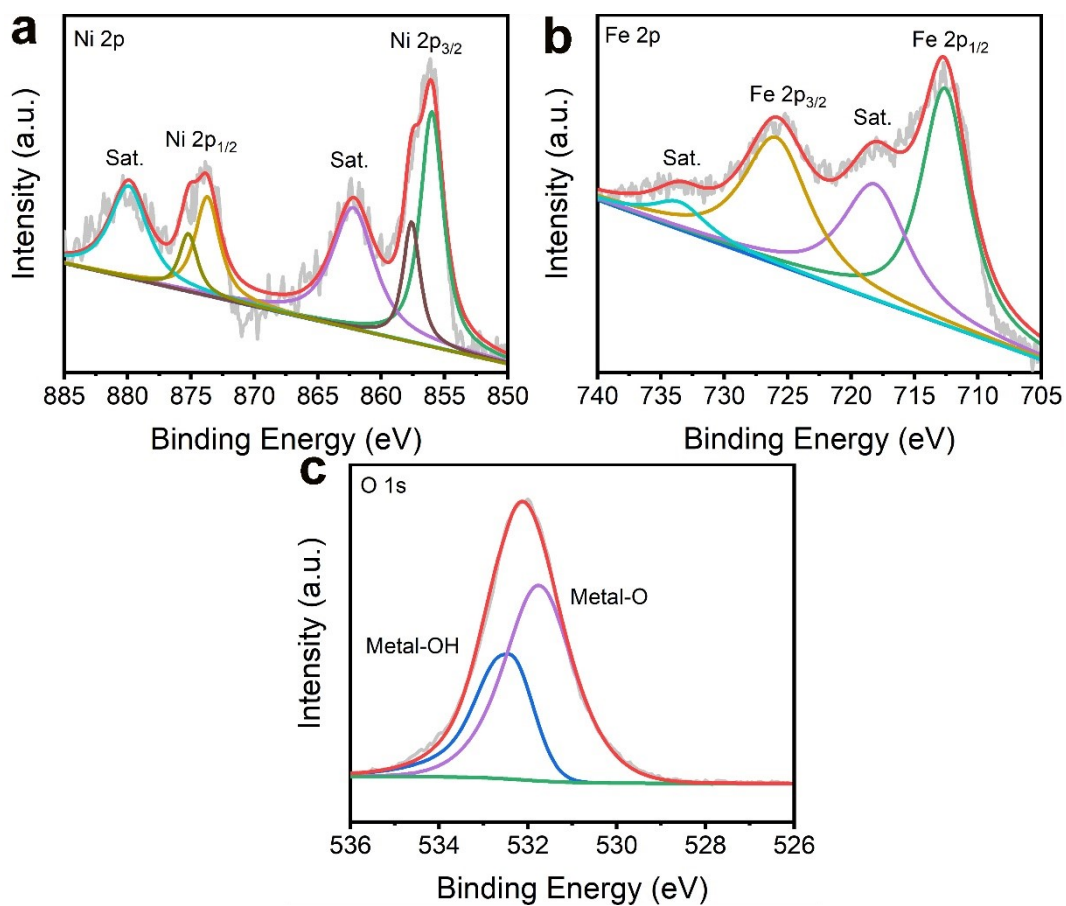


Fig. S17. XPS spectra in the (a) Ni 2p, (b) Fe 2p, and (c) O 1s regions for CoS₂@NiFe-LDH/CC after durability test in 1 M KOH + Seawater.

Table S1. Comparisons of the OER performance of CoS₂@NiFe-LDH/CC with other recently reported electrocatalysts in 1 M KOH.

Catalyst	Current density (mA cm ⁻²)	Overpotential (mV)	Electrolyte	Ref.
CoS ₂ @NiFe-LDH/CC	100	243	1 M KOH	This work
Ni ₂ Fe ₁ -LDH/NF	100	260	1 M KOH	1
NiCo ₂ S ₄ @CoNi-LDH/CC	100	377	1 M KOH	2
MnO _x /NiFe-LDH/NF	100	265	1 M KOH	3
Ni _{0.75} Fe _{0.15} Ce _{0.10} /NF	100	270	1 M KOH	4
Ni ₃ S ₂ /Cu-NiCo LDH/NF	100	304	1 M KOH	5
NiFe-LDH@NiFe-Bi/CC	100	336	1 M KOH	6
NiFe(OH) _x /Ni ₃ N/NF	100	290	1 M KOH	7
NiFe-LDH/Cu ₃ P	100	300	1 M KOH	8
NiO-Ni/NF	100	323	1 M KOH	9
NiCo ₂ S ₄ /CC	100	340	1 M KOH	10
Ni-Co-S/CF	100	363	1 M KOH	11
NiFe-MOF/NF	100	251	1 M KOH	12

Table S2. Comparisons of the OER performance of CoS₂@NiFe-LDH/CC with other recently reported electrocatalysts in alkaline simulated seawater or alkaline seawater.

Catalyst	Current density (mA cm ⁻²)	Overpotential (mV)	Electrolyte	Ref.
CoS ₂ @NiFe-LDH/CC	100	251	1 M KOH + 0.5 M NaCl	This work
	100	256	1 M KOH + Seawater	
AC-FeNi(O)OH	100	264	1 M KOH + Seawater	13
BZ-NiFe-LDH/CC	100	300	1 M KOH + Seawater	14
NiCoP/NiCo-LDH@NF	100	420	1 M KOH + 0.5 M NaCl	15
NiFeP/P-rGO/NF	100	290	1 M KOH + 1 M NaCl	16
Ni ₂ P-Fe ₂ P/NF	100	305	1 M KOH + Seawater	17
Ni(OH) ₂ -TCNQ/GP	100	340	1 M KOH + Seawater	18
Ni ₅ Co ₃ Mo-OH/NF	100	304	1 M KOH + Seawater	19
NiFe-LDH-6-4/CC	100	301	1 M KOH + Seawater	20
Fe-CoCH/NF	100	317	1 M KOH + Seawater	21
N-CDs/NiFeLDH/NF	100	285	1 M KOH + 0.5 M NaCl	22
		340	1 M KOH + Seawater	
ZnFe-BDC-0.75/NF	100	293	1 M KOH + 0.5 M NaCl	23
		308	1 M KOH + Seawater	
NiMoO ₄ @NiFe-LDH/NF	100	273	1 M KOH + 0.5 M NaCl	24
		315	1 M KOH + Seawater	

NiCoHPi@Ni ₃ N/NF	100	365	1 M KOH + 0.5 M NaCl	25
		396	1 M KOH + Seawater	
NiMoN@NiFeN/NF	100	286	1 M KOH + 0.5 M NaCl	26
		307	1 M KOH + Seawater	
Fe-Co-S/Cu ₂ O/Cu	100	390	1 M KOH + 0.5 M NaCl	27
		440	1 M KOH + Seawater	
S-(Ni,Fe)OOH/NF	100	278	1 M KOH + 0.5 M NaCl	28
		300	1 M KOH + Seawater	

References

- 1 L. Wang, D. Liu, Z. Zhang, Y. Li, J. Liu, Y. Yang, B. Xue and F. Li, *J. Alloys Compd.*, 2023, **934**, 167846.
- 2 F. Yuan, J. Wei, G. Qin and Y. Ni, *J. Alloys Compd.*, 2020, **830**, 154658.
- 3 Z. Wang, C. Wang, L. Ye, X. Liu, L. Xin, Y. Yang, L. Wang, W. Hou, Y. Wen and T. Zhan, *Inorg. Chem.*, 2022, **61**, 15256–15265.
- 4 J. Ding, Y. Han and G. Hong, *Int. J. Hydrogen Energy*, 2021, **46**, 2018–2025.
- 5 L. Jia, G. Du, D. Han, Y. Hao, W. Zhao, Y. Fan, Q. Su, S. Ding and B. Xu, *J. Mater. Chem. A*, 2021, **9**, 27639–27650.
- 6 L. Zhang, R. Zhang, R. Ge, X. Ren, S. Hao, F. Xie, F. Qu, Z. Liu, G. Du, A. M. Asiri, B. Zheng and X. Sun, *Chemistry. Eur. J.*, 2017, **23**, 11499–11503.
- 7 H. Zhang, X. Meng, J. Zhang and Y. Huang, *ACS Sustain. Chem. Eng.*, 2021, **9**, 12584–12590.
- 8 H. Wang, T. Zhou, P. Li, Z. Cao, W. Xi, Y. Zhao and Y. Ding, *ACS Sustain. Chem. Eng.*, 2017, **6**, 380–388.
- 9 Z. Yue, W. Zhu, Y. Li, Z. Wei, N. Hu, Y. Suo and J. Wang, *Inorg. Chem.*, 2018, **57**, 4693–4698.
- 10 D. Liu, Q. Lu, Y. Luo, X. Sun and A. M. Asiri, *Nanoscale*, 2015, **7**, 15122–15126.
- 11 T. Liu, X. Sun, A. M. Asiri and Y. He, *Int. J. Hydrogen Energy*, 2016, **41**, 7264–7269.
- 12 C.-Y. Tseng, I. C. Cheng and J.-Z. Chen, *Int. J. Hydrogen Energy*, 2022, **47**, 35990–35998.
- 13 R. Fan, X. Zhang, N. Yu, F. Wang, H. Zhao, X. Liu, Q. Lv, D. Liu, Y. Chai and B. Dong, *Inorg. Chem. Front.*, 2022, **9**, 4216–4224
- 14 L. Zhang, J. Liang, L. Yue, K. Dong, J. Li, D. Zhao, Z. Li, S. Sun, Y. Luo, Q. Liu, G. Cui, A. Ali Alshehri, X. Guo and X. Sun, *Nano Res. Energy*, 2022, **1**, e9120028.
- 15 Y. Wu, Z. Tian, S. Yuan, Z. Qi, Y. Feng, Y. Wang, R. Huang, Y. Zhao, J. Sun,

- W. Zhao, W. Guo, J. Feng and J. Sun, *Chem. Eng. J.*, 2021, **411**, 128538.
- 16 Q. Lei, L. Ang, W. Mei, Z. Yin, Z. Kai and L. Xinheng, *Adv. Mater. Interfaces*, 2021, **9**, 2101720.
- 17 L. Wu, L. Yu, F. Zhang, B. McElhenny, D. Luo, A. Karim, S. Chen and Z. Ren, *Adv. Funct. Mater.*, 2020, **31**, 2006484.
- 18 L. Zhang, J. Wang, P. Liu, J. Liang, Y. Luo, G. Cui, B. Tang, Q. Liu, X. Yan, H. Hao, M. Liu, R. Gao and X. Sun, *Nano Res.*, 2022, **15**, 6084–6090.
- 19 S. Hao, L. Chen, C. Yu, B. Yang, Z. Li, Y. Hou, L. Lei and X. Zhang, *ACS Energy Lett.*, 2019, **4**, 952–959.
- 20 G. Dong, F. Xie, F. Kou, T. Chen, F. Wang, Y. Zhou, K. Wu, S. Du, M. Fang and J. C. Ho, *Mater. Today Energy*, 2021, **22**, 100883.
- 21 S. Shi, S. Sun, X. He, L. Zhang, H. Zhang, K. Dong, Z. Cai, D. Zheng, Y. Sun, Y. Luo, Q. Liu, B. Ying, B. Tang, X. Sun and W. Hu, *Inorg. Chem.*, 2023, DOI: 10.1021/acs.inorgchem.3c01473.
- 22 P. Ding, H. Song, J. Chang and S. Lu, *Nano Res.*, 2022, **15**, 7063–7070.
- 23 Y. Cheng, Y. Luo, Y. Zheng, J. Pang, K. Sun, J. Hou, G. Wang, W. Guo, X. Guo and L. Chen, *Int. J. Hydrogen Energy*, 2022, **47**, 35655–35665.
- 24 H. Wang, L. Chen, L. Tan, X. Liu, Y. Wen, W. Hou and T. Zhan, *J. Colloid Interface Sci.*, 2022, **613**, 349–358.
- 25 H. Sun, J. Sun, Y. Song, Y. Zhang, Y. Qiu, M. Sun, X. Tian, C. Li, Z. Lv and L. Zhang, *ACS Appl. Mater. Interfaces*, 2022, **14**, 22061–22070.
- 26 L. Yu, Q. Zhu, S. Song, B. McElhenny, D. Wang, C. Wu, Z. Qin, J. Bao, Y. Yu, S. Chen and Z. Ren, *Nat. Commun.*, 2019, **10**, 5106.
- 27 J. Sun, P. Song, H. Zhou, L. Lang, X. Shen, Y. Liu, X. Cheng, X. Fu and G. Zhu, *Appl. Surf. Sci.*, 2021, **567**, 150757.
- 28 L. Yu, L. Wu, B. McElhenny, S. Song, D. Luo, F. Zhang, Y. Yu, S. Chen and Z. Ren, *Energy Environ. Sci.*, 2020, **13**, 3439–3446.